LAWRENCE
LIVERMORE
NATIONAL
LABORATORY

UCRL-PROC-211912

No-Core Shell Model and Reactions

P. Navratil, W. E. Ormand, E. Caurier, C. Bertulani

May 3, 2005

Reaction Mechanisms for Rare Isotope Beams
East Lansing, MI, United States
March 9, 2005 through March 12, 2005

No-Core Shell Model and Reactions

Petr Navrátil*, W. Erich Ormand*, Etienne Caurier† and Carlos Bertulani**

*Lawrence Livermore National Laboratory, L-414, P.O. Box 808, Livermore, CA 94551, USA
†Institut de Recherches Subatomiques, IN2P3-CNRS, Universite Louis Pasteur, F-67037 Strasbourg, France
**Department of Physics, University of Arizona, Tucson, AZ 85721

Abstract. There has been a significant progress in *ab initio* approaches to the structure of light nuclei. Starting from realistic two- and three-nucleon interactions the *ab initio* no-core shell model (NCSM) can predict low-lying levels in *p*-shell nuclei. It is a challenging task to extend *ab initio* methods to describe nuclear reactions. In this contribution, we present a brief overview of the NCSM with examples of recent applications as well as the first steps taken toward nuclear reaction applications. In particular, we discuss cross section calculations of p+^{6}Li and ^{6}He+p scattering as well as a calculation of the astrophysically important ^{7}Be(p,γ)^{8}B S-factor.

Keywords: Shell model; forces in hadronic systems and effective interactions; direct reactions; spectroscopic factors; radiative capture
PACS: 21.60.Cs, 21.30.Fe, 24.50.+g, 21.10.Jx, 25.40.Lw

1. INTRODUCTION

Various methods can be used to solve systems of three or four nucleons interacting by realistic interactions [1]. For $A > 4$ systems, a prominent approach has been the Green's function Monte Carlo (GFMC) method [2]. An alternative, and complementary, approach is the no-core shell model (NCSM) [3, 4, 5, 6, 7, 8, 9, 10]. It considers light nuclei as systems of A nucleons interacting by realistic inter-nucleon forces. The calculations are performed using a large but finite harmonic-oscillator (HO) basis. Due to the basis truncation, it is necessary to derive an effective interaction from the underlying inter-nucleon interaction. The effective interaction contains, in general, up to A-body components even if the underlying interaction had, e.g. only two-body terms. In practice, the effective interaction is derived in a sub-cluster approximation retaining just two- or three-body terms. A crucial feature of the method is its convergence to exact solution with the basis size increase and/or the effective interaction clustering increase.

Among successes of the NCSM approach was the first published result of the binding energy of ^{4}He with the CD-Bonn NN potential [6], and the first observation of incorrect ground-state spin in ^{10}B when realistic nucleon-nucleon interactions are employed [9, 11]. This last result is a new example, in addition to the under binding problem, for the need of realistic three-nucleon forces.

In this paper, we give a short overview of the NCSM theory in Sect. 2 with examples of recent results. In particular, we emphasize recent efforts to apply the nuclear structure information obtained within the NCSM to describe nuclear reactions. A derivation of the translationally invariant density from the NCSM wave functions is discussed in Sect. 3. The obtained density then serves as an input for the folding approaches to optical potentials used in the direct reaction coupled channel calculations. As examples of the application, the ^{6}Li and ^{6}He scattering on protons is investigated. Calculation of cluster form factors and spectroscopic factors is discussed in Sect. 4. In Sect. 5, we present preliminary results of the ^{7}Be(p,γ)^{8}B S-factor calculation from NCSM wave functions. Conclusions are given in Sect. 6.

2. *AB INITIO* NO-CORE SHELL MODEL

We consider a system of A point-like nonrelativistic nucleons that interact by realistic two- or two- plus three-nucleon interactions. As the simpler case when just the two-nucleon interaction is considered was discussed in many papers, see e.g. Ref. [8], we focus here on the more general case when both two- and three-nucleon interactions (TNI) are included. The starting Hamiltonian is then

$$H_A = \frac{1}{A}\sum_{i<j}\frac{(\vec{p}_i-\vec{p}_j)^2}{2m} + \sum_{i<j}^{A} V_{\mathrm{NN},ij} + \sum_{i<j<k}^{A} V_{\mathrm{NNN},ijk}\,, \tag{1}$$

where m is the nucleon mass, $V_{\mathrm{NN},ij}$ the NN interaction, $V_{\mathrm{NNN},ijk}$ the three-nucleon interaction. In the NCSM, we employ a large but finite HO basis. Due to properties of the realistic nuclear interaction in Eq. (1), we must derive an effective interaction appropriate for the basis truncation. To facilitate the derivation of the effective interaction, we modify the Hamiltonian (1) by adding to it the center-of-mass (CM) HO Hamiltonian $H_{\mathrm{CM}} = T_{\mathrm{CM}} + U_{\mathrm{CM}}$, where $U_{\mathrm{CM}} = \frac{1}{2}Am\Omega^2\vec{R}^2$, $\vec{R} = \frac{1}{A}\sum_{i=1}^{A}\vec{r}_i$. The effect of the HO CM Hamiltonian will later be subtracted out in the final many-body calculation. Due to the translational invariance of the Hamiltonian (1) the HO CM Hamiltonian has in fact no effect on the intrinsic properties of the system in the infinite basis space. The modified Hamiltonian can be cast into the form

$$\begin{aligned} H_A^{\Omega} &= H_A + H_{\mathrm{CM}} = \sum_{i=1}^{A} h_i + \sum_{i<j}^{A} V_{ij}^{\Omega,A} + \sum_{i<j<k}^{A} V_{\mathrm{NNN},ijk} = \sum_{i=1}^{A}\left[\frac{\vec{p}_i^{\,2}}{2m} + \frac{1}{2}m\Omega^2\vec{r}_i^{\,2}\right] \\ &\quad + \sum_{i<j}^{A}\left[V_{\mathrm{NN},ij} - \frac{m\Omega^2}{2A}(\vec{r}_i - \vec{r}_j)^2\right] + \sum_{i<j<k}^{A} V_{\mathrm{NNN},ijk}\,. \end{aligned} \tag{2}$$

Next we divide the A-nucleon infinite HO basis space into the finite active space (P) comprising of all states of up to $N_{\max}$ HO excitations above the unperturbed ground state and the excluded space ($Q = 1 - P$). The basic idea of the NCSM approach is to apply a unitary transformation on the Hamiltonian (2), $e^{-S}H_A^{\Omega}e^{S}$ such that $Qe^{-S}H_A^{\Omega}e^{S}P = 0$. If such a transformation is found, the effective Hamiltonian that exactly reproduces a subset of eigenstates of the full space Hamiltonian is given by $H_{\mathrm{eff}} = Pe^{-S}H_A^{\Omega}e^{S}P$. This effective Hamiltonian contains up to A-body terms and to construct it is essentially as difficult as to solve the full problem. Therefore, we apply this basic idea on a sub-cluster level. When a genuine TNI is considered, the simplest approximation is a three-body effective interaction approximation. The NCSM calculation is then performed with the following four steps:

(i) We solve a three-nucleon system for all possible three-nucleon channels with the Hamiltonian H_A^{Ω},i.e., using $h_1 + h_2 + h_3 + V_{12}^{\Omega,A} + V_{13}^{\Omega,A} + V_{23}^{\Omega,A} + V_{\mathrm{NNN},123}$. It is necessary to separate the three-body effective interaction contributions from the TNI and from the two-nucleon interaction. Therefore, we need to find three-nucleon solutions for the Hamiltonian with and without the $V_{\mathrm{NNN},123}$ TNI term. The three-nucleon solutions are obtained by procedures described in Refs. [7] (without TNI) and [12] (with TNI).

(ii) We construct the unitary transformation corresponding to the choice of the active basis space P from the three-nucleon solutions using the Lee-Suzuki procedure [13, 14]. The three-body effective interaction is then obtained as $V_{\mathrm{3eff},123}^{\mathrm{NN+NNN}} = P[e^{-S_{\mathrm{NN+NNN}}}(h_1 + h_2 + h_3 + V_{12}^{\Omega,A} + V_{13}^{\Omega,A} + V_{23}^{\Omega,A} + V_{\mathrm{NNN},123})e^{S_{\mathrm{NN+NNN}}} - (h_1 + h_2 + h_3)]P$ and $V_{\mathrm{3eff},123}^{\mathrm{NN}} = P[e^{-S_{\mathrm{NN}}}(h_1 + h_2 + h_3 + V_{12}^{\Omega,A} + V_{13}^{\Omega,A} + V_{23}^{\Omega,A})e^{S_{\mathrm{NN}}} - (h_1 + h_2 + h_3)]P$. The three-body effective interaction contribution from the TNI is then defined as $V_{\mathrm{3eff},123}^{\mathrm{NNN}} \equiv V_{\mathrm{3eff},123}^{\mathrm{NN+NNN}} - V_{\mathrm{3eff},123}^{\mathrm{NN}}$.

(iii) As the three-body effective interactions are derived in the Jacobi-coordinate HO basis but the A-nucleon calculations will be performed in a Cartesian-coordinate single-particle Slater-determinant m-scheme basis, we need to perform a suitable transformation of the interactions. This transformation is a generalization of the well-known transformation on the two-body level that depends on HO Brody-Moshinsky brackets.

(iv) We solve the Schrödinger equation for the A nucleon system using the Hamiltonian $H_{A,\mathrm{eff}}^{\Omega} = \sum_{i=1}^{A} h_i + \frac{1}{A-2}\sum_{i<j<k}^{A} V_{\mathrm{3eff},ijk}^{\mathrm{NN}} + \sum_{i<j<k}^{A} V_{\mathrm{3eff},ijk}^{\mathrm{NNN}}$, where the $\frac{1}{A-2}$ factor takes care of overcounting the contribution from the two-nucleon interaction. At this point we also subtract the H_{CM}. The A nucleon calculation is then performed using a shell model code generalized to handle three-body interactions.

An interesting example that demonstrates the importance of the TNI is the ground-state spin inversion in ^{10}B. The ground state of ^{10}B is $J^{\pi}T = 3^{+}0$. Calculations with the high-quality NN potenatials, however, predict a $1^{+}0$ ground state. [2, 9, 11] By including the Tucson-Melbourne TM$'$ TNI, the problem is resolved, see Fig. 1. In the figure, three parameter sets denoted as 81, 93 and 99 are considered for the TM$'$ TNI. All give similar results, dramatically different compared to the calculation with only the two-nucleon potential.

3. TRANSLATIONALLY INVARIANT DENSITY AND JLM OPTICAL POTENTIAL

In general, it is a challenging task to extend the *ab initio* methods to describe nuclear reactions. Concerning direct reactions, in particular the nucleon-nucleus elastic and inelastic scattering, a first and straightforward application of the NCSM is a semi-microscopic approach, e.g. the Jeukenne-Lejeune-Mahaux (JLM) [15], to construct optical potentials from the nuclear densities obtained in the NCSM. Eventually, these optical potentials can be used in coupled channels

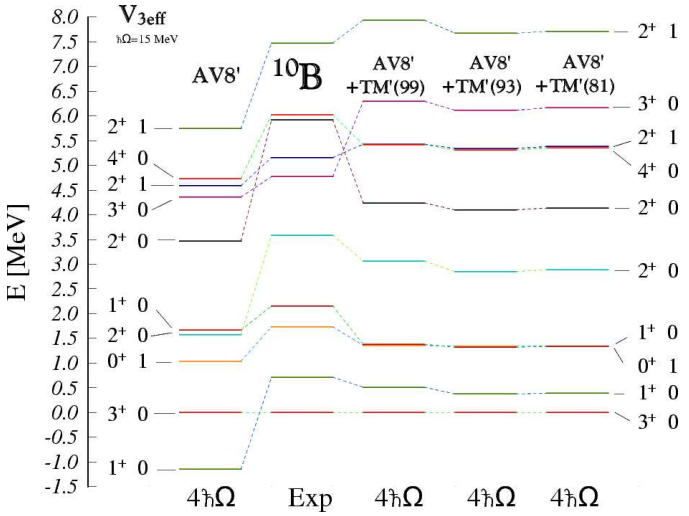

FIGURE 1. Excitation spectra of ^{10}B obtained using the AV8′ NN interactions and AV8′+TM′ interactions, respectively, are compared to experiment. Three parameter sets denoted as 81, 93 and 99 are considered for the TM′ TNI. The $4\hbar\Omega$ basis space and the $\hbar\Omega = 15$ MeV HO frequency were employed.

calculations by employing standard codes, e.g. Fresco [16]. To fully utilize NCSM nuclear structure for this purpose, the spurious CM contribution must be removed from the density.

The nuclear density operator is defined as [17]

$$\rho_{op}(\vec{r}) = \sum_{i=1}^{A} \delta(\vec{r} - \vec{r}_i) = \sum_{i=1}^{A} \frac{\delta(r - r_i)}{r r_i} \sum_m Y_{lm}(\hat{r}_i) Y^*_{lm}(\hat{r}) \; . \tag{3}$$

The physical density should depend on the coordinate measured from the CM of the nucleus, $\vec{r} - \vec{R}$. Using the transformation properties of the HO wave functions, it is possible to relate the physical density to the standard one-body density matrix elements (OBDME) computed in shell model codes from eigenstates obtained in the Slater determinant basis. The final expression is [18]

$$\begin{aligned} &\langle A\lambda_f J_f M_f | \rho_{op}(\vec{r} - \vec{R}) | A\lambda_i J_i M_i \rangle = (\tfrac{A}{A-1})^{3/2} \tfrac{1}{\hat{J}_f} \sum (J_i M_i K k | J_f M_f) Y^*_{Kk}(\widehat{\vec{r} - \vec{R}}) \\ \times \;& R_{nl}(\sqrt{\tfrac{A}{A-1}} |\vec{r} - \vec{R}|) R_{n'l'}(\sqrt{\tfrac{A}{A-1}} |\vec{r} - \vec{R}|) (-1)^K \frac{\hat{l}\hat{l}'(l0l'0|K0)}{\hat{l}_1 \hat{l}_2 (l_1 0 l_2 0 | K0)} (M^K)^{-1}_{nln'l', n_1 l_1 n_2 l_2} \\ \times \;& \langle l_1 \tfrac{1}{2} j_1 || Y_K || l_2 \tfrac{1}{2} j_2 \rangle \tfrac{-1}{\hat{K}} \, {}_{\rm SD}\langle A\lambda_f J_f || (a^\dagger_{n_1 l_1 j_1} \tilde{a}_{n_2 l_2 j_2})^{(K)} || A\lambda_i J_i \rangle_{\rm SD} \; , \end{aligned} \tag{4}$$

where the sum is restricted to both $l + l' + K$ and $l_1 + l_2 + K$ even. The λ_i and λ_f are the additional quantum numbers that classify the initial and final state, respectively. The matrix M^K is defined as

$$\begin{aligned} (M^K)_{n_1 l_1 n_2 l_2, nln'l'} \;=\; & \sum_{N_1 L_1} (-1)^{l+l'+K+L_1} \left\{ \begin{array}{ccc} l_1 & L_1 & l \\ l' & K & l_2 \end{array} \right\} \hat{l}\hat{l}' \\ & \times \; \langle nl00l | N_1 L_1 n_1 l_1 l \rangle_{\frac{1}{A-1}} \langle n'l'00l' | N_1 L_1 n_2 l_2 l' \rangle_{\frac{1}{A-1}} \; . \end{aligned} \tag{5}$$

As an illustration of the significance of the spurious CM removal, we calculated the ^{6}He physical (4) and the shell-model densities ${}_{\rm SD}\langle A\lambda_f J_f M_f | \rho_{op}(\vec{r}) | A\lambda_i J_i M_i \rangle_{\rm SD}$ using wave functions obtained in Ref. [19]. We note that the relationship between the Jacobi coordinate eigenstates appearing in Eq. (4) and the SD eigenstates is

$$\langle \vec{r}_1 \ldots \vec{r}_A | A\lambda JM \rangle_{\rm SD} = \langle \vec{\xi}_1 \ldots \vec{\xi}_{A-1} | A\lambda JM \rangle \varphi_{000}(\sqrt{A}\vec{R}) \; , \tag{6}$$

In Fig. 2, the proton and the neutron monopole ground state densities are shown. A $10\,\bar{h}\Omega$ basis space and the HO frequency of $\bar{h}\Omega = 13$ MeV was used. The two-body effective interaction was derived from the CD-Bonn NN potential.

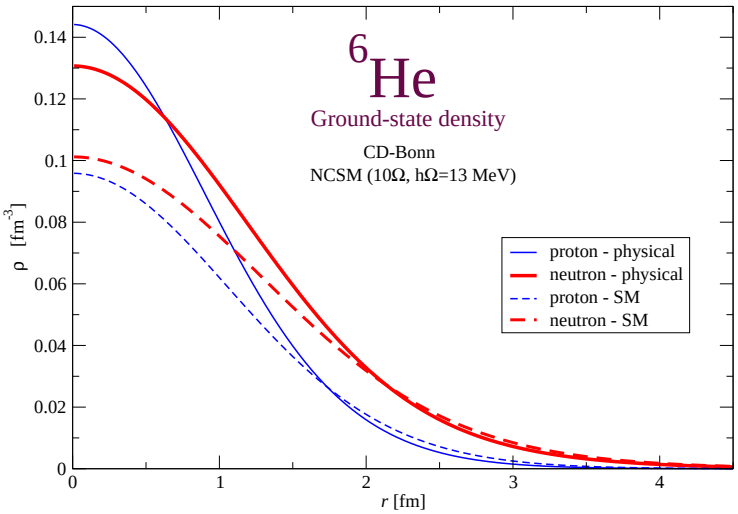

FIGURE 2. ^{6}He proton and neutron monopole ground state densities obtained in the $10\hbar\Omega$ basis space and the HO frequency of $\hbar\Omega = 13$ MeV. The NCSM two-body effective interaction was derived from the CD-Bonn NN potential. The full lines correspond to the physical densities calculated according to Eq. (4) while the dashed lines correspond to the shell-model densities that contain the spurious center-of-mass contribution.

The full lines correspond to the physical densities calculated according to Eq. (4) while the dashed lines correspond to the shell-model densities that contain the spurious CM contribution. Obviously, the same OBDME were employed in both calculations. The normalization of the densities in Fig. 2 is $4\pi \int drr^2 \rho_{K=0,p(n)}(r) = Z(N)$ with p, n refers to the proton and neutron, respectively, and $\rho_{K=0}(r) = \frac{1}{4\pi} \int d\hat{r} \, \langle A\lambda JM|\rho_{op}(\vec{r})|A\lambda JM\rangle$. Not surprisingly, a particularly signifi cant impact of the exact removal of the spurious CM motion is then found for the spin-orbit part of the optical potential proportional to the derivative of the nuclear density.

By multiplying the physical monopole densities by r^2 and integrating we obtain the point-proton and point-neutron rms radii 1.763 fm and 2.361 fm, respectively, identical to those calculated in Ref. [19] in a different way. Performing the same integral using the shell-model densities gives incorrect, larger radii 1.976 fm and 2.524 fm, respectively. The difference between the squares of the two sets of radii is equal to the mean value of the CM $\vec{R}^2$. It should be noted that a recent high-precision measurement of the ^{6}He proton radius reported a point-proton radius of 1.912(18) fm. [20] is larger than that we calculted in the $10\hbar\Omega$ model space with the HO frequency $\hbar\Omega = 13$ MeV. A more detailed investigation of the radius convergence is needed. For example, a new calculation in a larger space, $10\hbar\Omega$ and a different HO frequency $\hbar\Omega = 11$ MeV gives the point-proton radius 1.818 fm.

We performed differential cross sections calculations for the reactions p+^{6}Li at 72 MeV [21] and ^{6}He+p at 71 MeV/A [22]. Starting from the translationally invariant ground-state monopole densities obtained from $12\hbar\Omega$ NCSM calculations using the CD-Bonn NN potential, we constructed the JLM optical potential and the spin-orbit potential proportional to the derivative of the density. We employed the JLM parametrization from Ref. [23] with the local density approximation using the prescription with the mid-point interaction evaluation. Only the real part of the spin-orbit interaction was retained. A simultaneous χ-square fi t of the strength parameters of the real and imaginary central potential and the spin-orbit potential was performed for the two reactions. Our results are compared to experimental data in Fig. 3. The values of the fi tted parameters are $\lambda_V = 0.88, \lambda_W = 0.92$ and $\lambda_{so} = 0.80$.

4. CHANNEL CLUSTER FORM FACTOR CALCULATION

Detailed knowledge of nuclear structure is important for the description of low-energy nuclear reactions. As the fi rst step in the application of the NCSM to low-energy nuclear reactions, one needs to understand the cluster structure of the eigenstates. That is, one needs to calculate the channel cluster form factors. Those can then, e.g., be integrated to obtain the spectroscopic factors. Let's consider a composite system of A nucleons, a projectile of a nucleons and a target of $A-a$ nucleons. All the nuclei are assumed to be described by eigenstates of the NCSM effective Hamiltonians expanded in the HO basis with identical HO frequency and the same (for the eigenstates of the same parity) or differing

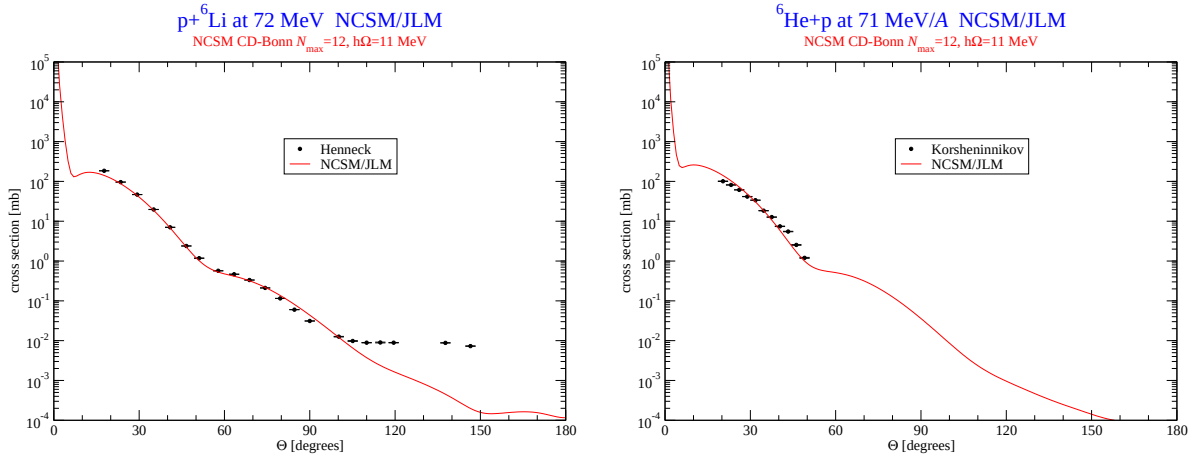

FIGURE 3. Differential cross section for p+^{6}Li at 72 MeV (left) and for ^{6}He+p at 71 MeV/A (right). The NCSM densities obtained in a $12\hbar\Omega$ calculation were used to generate the JLM optical potentials. Experimental data are from Refs. [21] and [22], respectively.

by one unit of the HO excitation (for the eigenstates of opposite parity) definitions of the model space. We limit ourselves to $a \leq 4$ projectiles. In such a case, the projectiles can be efficiently described by a Jacobi-coordinate HO wave functions. The target and the composite system is assumed to be described by Slater determinant single-particle HO basis wave functions which is in general more efficient for $A > 4$. Let us introduce a projectile-target wave function

$$\begin{aligned} & \langle \vec{\xi}_1 \dots \vec{\xi}_{A-a-1} \eta'_{A-a} \hat{\eta}_{A-a} \vec{\vartheta}_{A-a+1} \dots \vec{\vartheta}_{A-1} | \Phi^{(A-a,a)JM}_{\alpha I_1,\beta I_2;sl}; \delta_{\eta_{A-a}} \rangle \\ = & \sum (I_1 M_1 I_2 M_2 | s m_s)(s m_s l m_l | J M) \frac{\delta(\eta_{A-a} - \eta'_{A-a})}{\eta_{A-a}\eta'_{A-a}} Y_{l m_l}(\hat{\eta}_{A-a}) \\ \times & \langle \vec{\xi}_1 \dots \vec{\xi}_{A-a-1} | A-a \alpha I_1 M_1 \rangle \langle \vec{\vartheta}_{A-a+1} \dots \vec{\vartheta}_{A-1} | a \beta I_2 M_2 \rangle \ , \end{aligned} \tag{7}$$

The calculation of the cluster form factor

$$\begin{aligned} & g^{A\lambda JT}_{A-a\alpha I_1,a\beta I_2;sl}(\eta_{A-a}) = \langle A\lambda J | \mathscr{A} \Phi^{(A-a,a)J}_{\alpha I_1,\beta I_2;sl}; \delta_{\eta_{A-a}} \rangle \\ = & \sqrt{\frac{A!}{(A-a)!a!}} \sum_n R_{nl}(\eta_{A-a}) \langle A\lambda J | \Phi^{(A-a,a)J}_{\alpha I_1,\beta I_2;sl}; nl \rangle \ , \end{aligned} \tag{8}$$

can then be done in two steps. First, using the relation (6) for both the composite and the target eigenstate and the HO wave function transformations we obtain

$$_{\rm SD}\langle A\lambda J | \mathscr{A} \Phi^{(A-a,a)J}_{\alpha I_1,\beta I_2;sl}; nl \rangle_{\rm SD} = \langle nl00l | 00nll \rangle_{\frac{a}{A-a}} \ \langle A\lambda J | \mathscr{A} \Phi^{(A-a,a)J}_{\alpha I_1,\beta I_2;sl}; nl \rangle \ , \tag{9}$$

with a general HO bracket due to the CM motion. The nl in (8) and (9) refers to a replacement of $\delta_{\eta_{A-a}}$ by the HO $R_{nl}(\eta_{A-a})$ radial wave function. Second, we relate the SD overlap to a linear combination of matrix elements of a creation operators between the target and the composite eigenstates $_{\rm SD}\langle A\lambda J | a^\dagger_{n_1 l_1 j_1} \dots a^\dagger_{n_a l_a j_a} | A-a\alpha I_1 \rangle_{\rm SD}$. Such matrix elements are easily calculated by shell model codes. To obtain the channel cluster form factor we use the second equality in Eq. (8). The spectroscopic factor is obtained by integrating the square of the form factor.

As an example, we present results for the ^{7}Li$\rightarrow^4$He+t channel cluster form factors in Fig. 4. Apart from the large overlap integrals and spectroscopic factors for the bound $\frac{3}{2}^-_1$ and $\frac{1}{2}^-_1$ states, we find these quantities to be large also for the first excited $\frac{7}{2}^-_1$ and the first excited $\frac{5}{2}^-_1$ state. Both these states appear as resonances in the ^{4}He+t cross section. [24] The present results can be compared to the three-nucleon transfer calculations of Ref. [25] obtained using the phenomeological Cohen-Kurath interaction. [26] The agreement for the lowest four states is quite good. For the second excited $\frac{5}{2}^-_2$ state, however, our spectroscopic factor is significantly smaller than the one obtained in Ref.

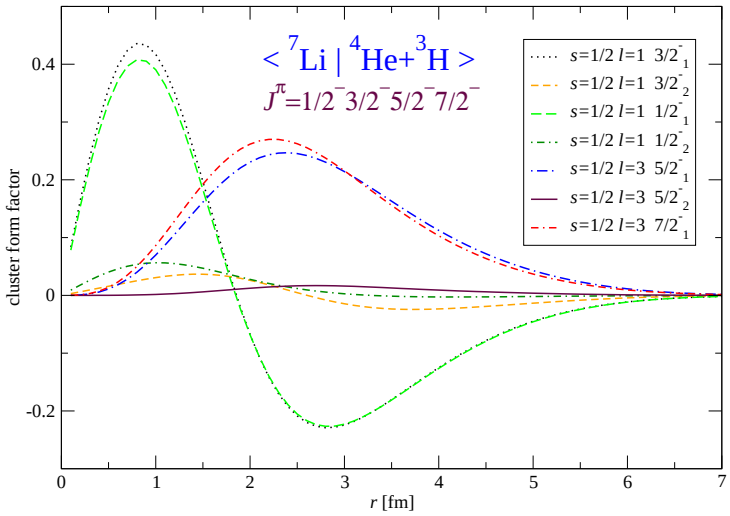

FIGURE 4. Overlap integral, g(r), of the ^{7}Li low-lying $J = \frac{1}{2}^-, \frac{3}{2}^-, \frac{5}{2}^-, \frac{7}{2}^-$ states with the ^{4}He+^{3}H as a function of separation between the ^{4}He and the triton. The CD-Bonn 2000 NN potential, the basis size of $N_{\max} = 8$ (for ^{7}Li), $N_{\max} = 10$ (for ^{4}He and ^{3}H) and the HO frequency of $\hbar\Omega = 13$ MeV were used.

[25]. The other system involving ^{7}Li as the composite nucleus that we investigated is ^{6}Li+n. As in the ^{7}Li$\rightarrow^4$He+t case, we observe large overlap integrals and spectroscopic factors for the two bound states $\frac{3}{2}^-_1$ and $\frac{1}{2}^-_1$. Contrary to the ^{7}Li$\rightarrow^4$He+t case, however, we find a large overlap integral and the spectroscopic factor for the $\frac{5}{2}^-_2$ state. The lowest $\frac{7}{2}^-_1$ and $\frac{5}{2}^-_1$ states have negligible overlap integrals for the ^{6}Li+n system. The large overlap integral and the spectroscopic factor for the $\frac{5}{2}^-_2$ state is consistent with the observed resonance in the ^{6}Li+n cross section.

5. ^{7}BE(P,γ)^{8}B S-FACTOR FROM NCSM WAVE FUNCTIONS

The ^{7}Be(p,γ)^{8}B capture reaction serves as an important input for understanding the solar neutrino flux [27]. S-factor of this reaction needs to be known with a precision of better than 9%. Current experimental uncertainties are around 20%. Many theoretical investigations were devoted to this reaction. Here we present a calculation for the S-factor starting from the *ab initio* NCSM wave functions for ^{8}B and ^{7}Be. The NCSM calculations were performed using the CD-Bonn NN potential in the model spaces up to $10\hbar\Omega$ for both nuclei. The harmonic oscillator frequency $\hbar\Omega = 12$ MeV, which produces the ground-state energy minimum in the $10\hbar\Omega$ space, was selected as the starting point also for the present S-factor calculation. The ground-state wave functions for ^{8}B and ^{7}Be were utilized to calculate the cluster form factors or overlap integrals that serve as the S-factor calculation input. The two most important channels are the p-waves, $l = 1$, with the proton in the $j = 3/2$ and $j = 1/2$ states, $\vec{j} = \vec{l} + \vec{s}, s = 1/2$. In these channels, we obtain the spectroscopic factors of 0.96 and 0.10, respectively. The dominant $j = 3/2$ overlap integral is presented in the left of Fig. 5 by the full line. Despite the fact, that a very large basis was employed in the present calculation, it is aparent that the overlap integral is nearly zero at about 10 fm. This is a consequence of the HO basis asymptotics. The proton capture on ^{7}Be to the weakly bound ground state of ^{8}B associated dominantly by the $E1$ radiation is a peripheral process. Consequently, the overlap integral with an incorrect asymptotic behavior cannot be used to calculate the S-factor.

It is our expectation, however, that the interior part of the overlap integral as obtained from our large-basis NCSM calculation is realistic. It is straightforward then to correct the asymptotic behavior of the overlap integral. We performed a least-square fit of a Woods-Saxon potential solution to the interior of the NCSM overlap in the range of $0-4$ fm. The Woods-Saxon potential parameters were varied in the fit under the constrain that the experimental separation energy of ^{7}Be+p was reproduced. In this way we obtain a perfect fit to the interior of the overlap integral and a correct asymptotic behavior at the same time. The resulting overlap is presented in Fig. 5 by the dashed line. Eventually, we rescale the overlap to preserve the original NCSM spectroscopic factor. The same procedure is applied

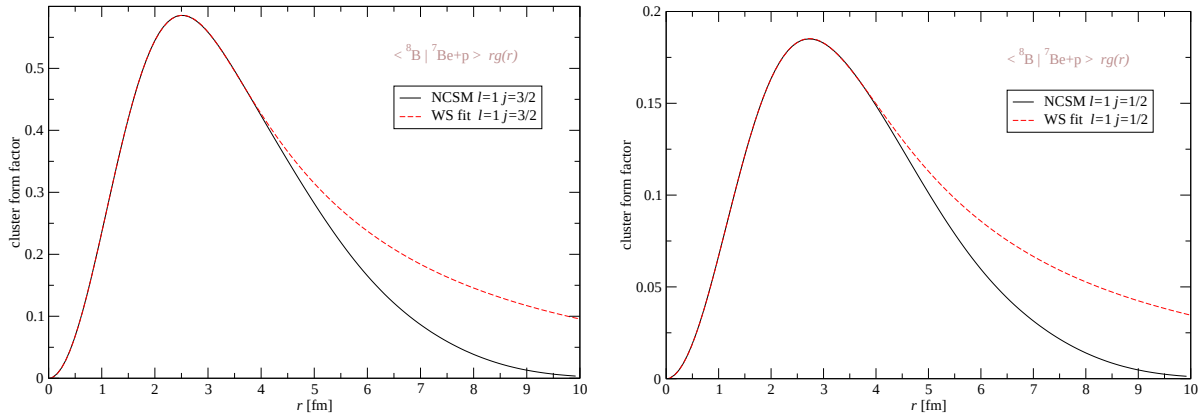

FIGURE 5. Overlap integral, $rg(r)$, for the ground state of ^{8}B with the ground state of ^{7}Be plus proton as a function of separation between the ^{7}Be and the proton. Left (right), the *p*-wave channel with $j = 3/2$ ($j = 1/2$) is shown. The full line represents the NCSM result, while the dashed line represents a renormalized overlap obtained from a Woods-Saxon potential whose parameters were fit to the NCSM overlap up to 4.0 fm under the constraint to reproduce the experimental separation energy.

to the other *p*-wave channel (right panel in Fig. 5). Obviously, the Woods-Saxon parameters obtained for the two channels are different. The corrected overlap integrals then serve as the input for the S-factor calculation performed as described in Ref. [28]. The scattering ^{7}Be+p *s*- and *d*-wave states are obtained within the potential model approach using a Woods-Saxon potential used in Ref. [29].

Our obtained S-factor is presented in Figs. 6 where contribution from the two partial waves are shown together with the total result (left figure). It is interesting to note a good agreement of our calculated S-factor with the recent Seattle direct measurement [30]. The sensitivity of the S-factor to the size of the NCSM basis is also presented in Figs. 6 (right figure). The overlap integrals were obtained in 6, 8 and 10 $\hbar\Omega$ calculations and independently corrected to insure the proper asymptotic behavior. The same scattering states were used in all three cases. It is aparent that the sensitivity to the basis change is rather moderate. We observe a small oscillation at this frequency ($\hbar\Omega = 12$ MeV). More detailed inverstigation of the basis size and the HO frequency sensitivity is under way.

6. CONCLUSION

Substantial progress has been made towards an exact description of nuclear structure. In this work, we described the *ab initio* no-core shell model and recent results. In particular, we find that realistic NN interactions by themselves are inadequate and that three-nucleon forces play an important role in determining nuclear properties. We are also in the process of extending the no-core shell model into a formalism capable of providing a description of nuclear reactions. Overall, the prospects are good that exact results for both structure and reactions for nuclei up to Oxygen utilizing the fundamental forces between nucleons can be achieved in the near future.

ACKNOWLEDGMENTS

We thank I. Thompson for assistance and help with the direct reaction code Fresco as well as with the code for constructing the JLM optical potential. This work was performed under the auspices of the U. S. Department of Energy by the University of California, Lawrence Livermore National Laboratory under contract No. W-7405-Eng-48. Support from the LDRD contract No. 04-ERD-058 is acknowledged.

REFERENCES

1. J. L. Friar *et al.*, *P*hys. Lett. **B 311**, 4 (1993); W. Glöckle and H. Kamada, *P*hys. Rev. Lett. **71**, 971 (1993); M. Viviani, A. Kievsky, and S. Rosati, *F*ew-Body Systems **18**, 25 (1995).

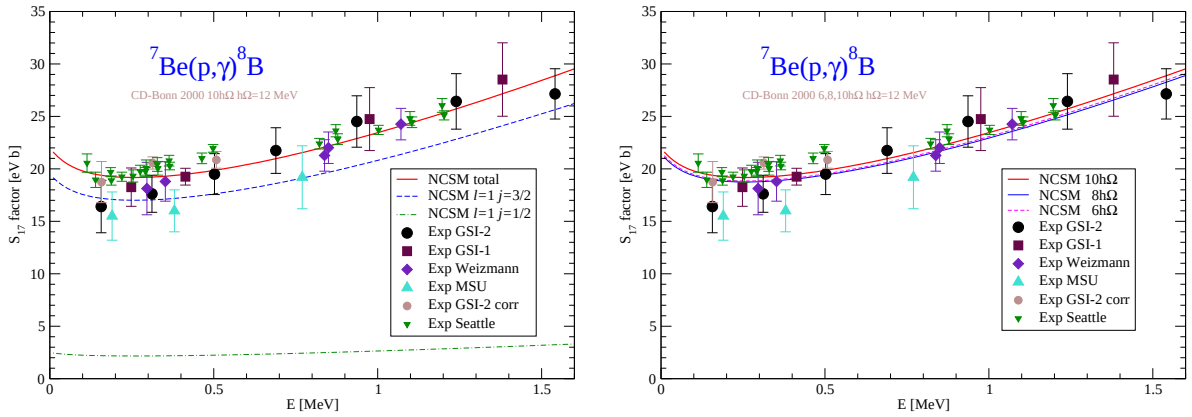

FIGURE 6. The ^{7}Be(p,γ)^{8}B S-factor obtained using the NCSM cluster form factors with corrected asymptotics as described in the text. Left, the dashed and dashed-dotted lines show the contribution due to the $l = 1$, $j = 3/2$ and $j = 1/2$ partial waves, respectively. Right, the dependence on the size of the basis form $6\hbar\Omega$ to $10\hbar\Omega$ is shown. Experimental values are from Refs. [30, 31].

2. B. S. Pudliner *et al.*, *P*hys. Rev. C **56** 1720, (1997); R. B. Wiringa, *N*ucl. Phys. **A 631**, 70c (1998); R. B. Wiringa *et al.*, *P*hys. Rev. C **62**, 014001 (2000); S. C. Pieper *et al.*, *P*hys. Rev. C **64**, 014001 (2001).
3. D. C. Zheng, B. R. Barrett, L. Jaqua, J. P. Vary and R. J. McCarthy, *P*hys. Rev. C **48**, 1083 (1993); D. C. Zheng, J. P. Vary, and B. R. Barrett, *P*hys. Rev. C **50**, 2841 (1994); D. C. Zheng, B. R. Barrett, J. P. Vary, W. C. Haxton and C.-L. Song, *P*hys. Rev. C **52**, 2488 (1995).
4. P. Navrátil and B. R. Barrett, *P*hys. Rev. C **54**, 2986 (1996).
5. P. Navrátil and B. R. Barrett, *P*hys. Rev. C **57**, 562 (1998).
6. P. Navrátil and B. R. Barrett, *P*hys. Rev. C **59**, 1906 (1999).
7. P. Navrátil, G. P. Kamuntavičius and B. R. Barrett, *P*hys. Rev. C **61**, 044001 (2000).
8. P. Navrátil, J. P. Vary and B. R. Barrett, *P*hys. Rev. Lett. **84**, 5728 (2000); *P*hys. Rev. C **62**, 054311 (2000).
9. P. Navrátil and W. E. Ormand, *P*hys. Rev. Lett. **88**, 152502 (2002).
10. P. Navrátil and W. E. Ormand, *P*hys. Rev. C **68**, 034305 (2003).
11. E. Caurier, P. Navrátil, W. E. Ormand and J. P. Vary, *P*hys. Rev. C **66**, 024314 (2002).
12. D. C. J. Marsden, P. Navrátil, S. A. Coon and B. R. Barrett, *P*hys. Rev. C **66**, 044007 (2002).
13. K. Suzuki and S. Y. Lee, *P*rog. Theor. Phys. **64**, 2091 (1980).
14. K. Suzuki and R. Okamoto, *P*rog. Theor. Phys. **92**, 1045 (1994).
15. J.-P. Jeukenne, A. Lejeune and C. Mahaux, *P*hys. Rev. C **16**, 80 (1977).
16. I. J. Thompson, *C*omputer Physics Reports **7**, 167 (1988).
17. G. R. Satchler, *D*irect Nuclear Reactions, Oxford University Press 1983.
18. P. Navrátil, *P*hys. Rev. C **70**, 014317 (2004).
19. P. Navrátil, J. P. Vary, W. E. Ormand and B. R. Barrett, *P*hys. Rev. Lett. 87, 172502 (2001).
20. L.-B. Wang *et al*. *P*hys. Rev. Lett. **93**, 142501 (2004).
21. R. Henneck *et al.*, *N*ucl. Phys. **A571**, 541 (1994).
22. A. A. Korsheninnikov *et al.*, *N*ucl. Phys. **A 617**, 45 (1997).
23. E. Bauge, J. P. Delaroche and M. Girod, *P*hys. Rev. C **58**, 1118 (1998).
24. D. R. Tilley, C. M. Cheves, J. L. Godwin, G. M. Hale, H. M. Hofmann, J. H. Kelley, C. G. Sheu and H. R. Weller, *N*ucl. Phys. **A 708**, 3 (2002).
25. D. Kurath and D. J. Millener, Nucl. Phys. **A238** 269, (1975).
26. S. Cohen and D. Kurath, *N*ucl. Phys. **73** 1, (1965).
27. E. Adelberger it et al., *R*ev. Mod. Phys. **70**, 1265 (1998).
28. C. Bertulani, *C*omp. Phys. Comm. **156**, 123 (2003).
29. H. Esbensen and G. F. Bertsch, *N*ucl. Phys. **A 600**, 37 (1996).
30. A. R. Junghans, E. C. Mohrmann, K. A. Snover, T. D. Steiger, E. G. Adelberger, J. M. Casandjian, H. E. Swanson, L. Buchmann, S. H. Park, A. Zyuzin, and A. M. Laird, *P*hys. Rev. C **68**, 065803 (2003).
31. N. Iwasa *et al.*, *P*hys. Rev. Lett. **83**, 2910 (1999); B. Davids *et al.*, *P*hys. Rev. Lett. **86**, 2750 (2001); L.T. Baby *et al.*, *P*hys. Rev. Lett. **90**, 022501 (2003); F. Schuemann *et al.*, *P*hys. Rev. Lett. **90**, 232501 (2003).